Structure and enzymatic properties of an unusual cysteine tryptophylquinone-dependent glycine oxidase from *Pseudoalteromonas luteoviolacea*

Andres Andreo-Vidal[1], **Kyle J. Mamounis**[2], **Esha Sehanobish**[2,#], **Dante Avalos**[3], **Jonatan Cristian Campillo-Brocal**[1], **Antonio Sanchez-Amat**[1], **Erik T. Yukl**[3], and **Victor L. Davidson**[2,*]

[1]Department of Genetics and Microbiology, University of Murcia, Murcia 30100, Spain

[2]Burnett School of Biomedical Sciences, College of Medicine, University of Central Florida, Orlando, FL 32827 United States

[3]Department of Chemistry and Biochemistry, New Mexico State University, Las Cruces, NM 88003

Abstract

Glycine oxidase from *Pseudoalteromonas luteoviolacea* (PlGoxA) is a cysteine tryptophylquinone (CTQ)-dependent enzyme. Sequence and phylogenetic analysis place it in a newly designated subgroup (Group IID) of a recently identified family of LodA-like proteins, which are predicted to possess CTQ. The crystal structure of PlGoxA reveals that it is a homo-tetramer. It possesses an N-terminal domain with no close structural homologues in the Protein Data Bank. The active site is quite small due to intersubunit interactions, which may account for the observed cooperativy towards glycine. Steady-state kinetic analysis yielded values of k_{cat}=6.0±0.2 s^{-1}, $K_{0.5}$=187±18 μM and h=1.77±0.27. In contrast to other quinoprotein amine dehydrogenases and oxidases that exhibit anomalously large primary kinetic isotope effects on the rate of reduction of the quinone cofactor by the amine substrate, no significant primary kinetic isotope effect was observed for this reaction of PlGoxA. The absorbance spectrum of the glycine-reduced PlGoxA exhibits features in the 400-650 nm range that have not previously been seen in other quinoproteins. Thus, in addition to the unusual structural features of PlGoxA, the kinetic and chemical reaction mechanisms of the reductive half-reaction of PlGoxA appear to be distinct from those of other amine dehydrogenases and amine oxidases that use tryptophylquinone and tyrosylquinone cofactors.

Graphical abstract

---

*Corresponding authors**: Victor L. Davidson, Burnett School of Biomedical Sciences, College of Medicine, University of Central Florida, 6900 Lake Nona Blvd., Orlando, FL 32827 Tel: 407-266-7111. Fax: 407-266-7002. victor.davidson@ucf.edu.
#**Present Address** Esha Sehanobish: Department of Biochemistry, Albert Einstein College of Medicine, New York, NY 10461. Email: esha.sehanobish@einstein.yu.edu
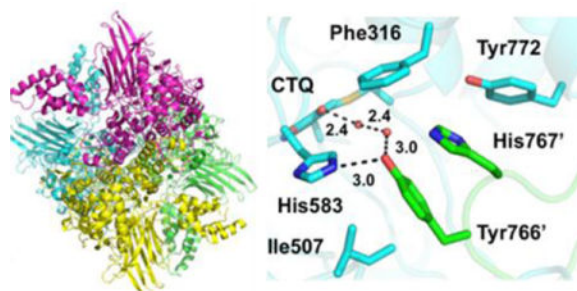
Supporting Information
Figure S1. Phylogenetic relationships of GoxA-like proteins in Group II.

Author Contributions
The manuscript was written through contributions of all authors. All authors have approved the final version of the manuscript.

Notes
The authors declare no competing financial interest.

INTRODUCTION

Quinoproteins are a family of enzymes that utilize a quinone species in the active site. A number of quinoprotein dehydrogenases have been described that contain either an exogenous pyrroloquinoline quinone (PQQ) cofactor [1] or various protein-derived quinone cofactors formed by irreversible posttranslational modifications [2, 3]. Copper-containing amine oxidases contain trihydroxyphenylalanine (topaquinone or TPQ) in which two oxygen atoms are inserted into a Tyr residue [4, 5]. Lysyl oxidase contains lysine tyrosylquinone in which one oxygen atom is inserted into a Tyr residue, which is also covalently cross-linked to a Lys side chain [6]. Two tryptophylquinone cofactors have also been characterized (Figure 1). Tryptophan tryptophylquinone (TTQ) is present in amine dehydrogenases [1, 3] and consists of a di-oxygenated Trp side-chain crosslinked to another Trp residue [7]. Cysteine tryptophylquinone (CTQ) is present in quinohemoprotein amine dehydrogenase (QHNDH). It is similar to TTQ except that a Cys sulfur is crosslinked to the di-oxygenated Trp residue [8].

Recently, a group of quinoproteins called LodA-like proteins was identified that utilize a CTQ cofactor for oxidase activity. The first member of this group to be described was LodA from *Marinomonas mediterranea*, a lysine ε-oxidase [9]. The second member to be described was GoxA from *M. mediterranea* (MmGoxA), which is a glycine oxidase [10, 11]. These are the only enzymes known to utilize a tryptophylquinone for oxidase activity. Furthermore, in contrast to the LodA-like proteins, all other known amino acid oxidases are flavoenzymes [12].

The biosynthesis of CTQ requires the product of a gene that is present in the same operon and predicted to encode a flavoprotein. For LodA it is *lodB* [13] and for MmGoxA it is Mm*goxB* [14]. All LodA-like proteins are predicted from sequence comparison to possess the CTQ cofactor and have a distinct evolutionary origin [15]. Genes predicted to encode LodA-like proteins are present in approximately 1% of sequenced microbial genomes, including several classes of bacteria and fungi. In each case, a gene similar to *lodB* and Mm*goxB* is also present. Thus, the LodA-like proteins are also the only class of quinoproteins that require a flavoenzyme for the post-translational biosynthesis of the protein-derived quinone cofactor.

A phylogenetic analysis of sequences of predicted LodA-like proteins revealed that they could be clustered in five major groups [15]. LodA is in Group I and MmGoxA is in Group II. In the original phylogenetic analysis reported in 2015, Group II contained 19 LodA-like

proteins. The topic of this study is the detection and analysis of a novel GoxA from *Pseudoalteromonas luteoviolacea* CPMOR-2 (PlGoxA). The genus *Pseudoalteromonas* includes different species with genes encoding LodA-like proteins. In the case of *P. luteoviolacea* CPMOR-2, the synthesis of L-amino acid oxidases has been reported [16]. The genome of this strain has been recently sequenced (GCA_001625645.1). Genome mining revealed that this strain contains a gene with similarity to Mm*goxA*. Present with Pl*goxA* gene is a *lodB*-like gene (Pl*goxB*), in accordance with these genes comprising a LodA-like operon. A new phylogenetic analysis is presented herein, which includes this bacterium and other genomes that have since been added to the database. It reveals that the Group II of LodA-like proteins now contains 77 proteins that can be clearly divided into four well-defined subgroups. MmGoxA resides in Group IIA and PlGoxA resides in Group IID.

In addition to the sequence and phylogenetic analyses, in the current study PlGoxA was expressed in and purified from *E. coli*. A high-resolution crystal structure was determined and the physical, kinetic and spectroscopic properties of PlGoxA were characterized. The results reveal that PlGoxA is a glycine oxidase that exhibits interesting distinctions from MmGoxA and LodA, and the TTQ- and CTQ-bearing dehydrogenases. Its properties are also distinct from traditional glycine oxidases that utilize a flavin cofactor.

EXPERIMENTAL PROCEDURES

Detection of LodA-like proteins

The tools available at Integrated Microbial Genomes Expert Review (IMG/MER) [17] were used for the detection of LodA-like proteins. MmGoxA (accession number ADZ90918) was used to search the database. Genes encoding similar proteins with an E-value lower than 1e^{-20} were identified using BLASTP search at IMG/MER. As a result, 500 proteins including PlGoxA were identified and selected for phylogenetic analysis. Sequence and phylogenetic analyses. LodA-like proteins were aligned with MUSCLE (MUltiple Sequence Comparison by Log-Expectation) [18] and evolutionary analysis were conducted using the software MEGA6 [19]. Phylogenetic relationships were inferred using the Neighbor-Joining (NJ) method, where the distances between sequences were computed using the p-distance method and are in the units of the number of amino acid differences per site. The reliability of each node in the tree constructed was estimated using bootstrap analysis with 500 replicates. Different phylogenetic groups, meeting the criterion of being supported by bootstrap values higher than 70%, were established.
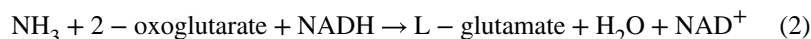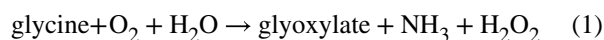
Expression and purification of PlGoxA

The gene cluster containing Pl*goxA* and Pl*goxB* was amplified from genomic DNA of *P. luteoviolacea* CPMOR-2 using the primers PlGoxACPMOR2Nde (D) 5′-TATTAAGGACAAcatATGTCAAATTGTCAG-3′ and PlGoxBCPMOR2AXho (R) 5′-GAAGTGCCTTATCTcgAGCCTAGA-3′, (the residues modified are in lower case and the restriction sites are underlined). The product of the PCR was cloned into a pET15b vector with an N-terminal hexahistidine tag on Pl*goxA*. The genes were expressed in *E. coli* Rosetta cells. The cells were grown in LB media, which also contained ampicillin and chloramphenicol, and the cells were induced with 1 mM IPTG for four h at 30 °C prior to

harvesting. The cells were disrupted by sonication and the cell extract was applied to a Ni-NTA affinity column. The protein eluted over a range of 30-150 mM imidazole. Purity of the protein was ascertained by SDS-PAGE.

Steady-state kinetics

Glycine oxidase activity was assayed using a previously described coupled-enzyme assay [11] in which the formation of the NH_3 that is released from glycine (eq 1), is monitored by coupling its production to the reaction of glutamate dehydrogenase (eq 2). The standard assay mixture contained 0.5 μM PlGoxA, 5 mM 2-oxoglutarate, 0.25 mM NADH, and 20 U/ml glutamate dehydrogenase. Reactions were performed in 50 mM potassium phosphate, pH 7.5, at 30°C. Initial velocity was determined by monitoring the rate of disappearance of NADH at 340 nm using the ε_{340} of NADH of 6220 $M^{-1}cm^{-1}$. Experiments were performed either with either aerobic buffer ($[O_2]$=252 μM) or O_2-saturated buffer ($[O_2]$=1150 μM). Data were analyzed by the Michaelis-Menten equation (eq 3) and the Hill equation (eq 4) in which h is the Hill coefficient. Standard errors were determined from a minimum of two replicates from different experiments using the same prep, as well as experiments using protein from at least two different preps.
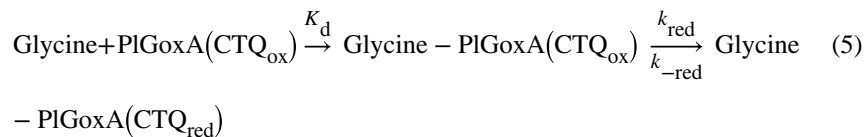
$$glycine + O_2 + H_2O \rightarrow glyoxylate + NH_3 + H_2O_2 \quad (1)$$

$$NH_3 + 2-oxoglutarate + NADH \rightarrow L-glutamate + H_2O + NAD^+ \quad (2)$$

$$v/[E] = k_{cat}[S]/(K_m + [S]) \quad (3)$$

$$v/[E] = k_{cat}[S]^h/((K_{0.5})^h + [S]^h) \quad (4)$$

Single-turnover kinetics

The rate of reduction of PlGoxA by glycine was monitored using an On-Line Instruments (OLIS, Bogart, GA) RSM1000 stopped-flow rapid scanning spectrophotometer. Experiments were performed in 50 mM potassium phosphate, pH 7.5, at 30 °C. The limiting reactant, 20 μM PlGoxA, was mixed with varying excess concentrations of glycine or glycine-d_5 (Sigma Chemical). After rapid mixing the reactions were monitored over the range from 300 to 530 nm to observe the conversion of CTQ to substrate-reduced CTQ. Kinetic data were reduced by factor analysis using the singular-value decomposition (SVD) algorithm and then globally fit using the fitting routines of OLIS Global Fit. Kinetic data were analyzed using the model described in eq 5. In each of the single-turnover kinetic experiments, the observed rate constant (k_{obs}) was best fit to a single-exponential relaxation.

The limiting first-order rate constant for the reduction of CTQ (k_{red}) was determined from the concentration dependence of k_{obs} using eq 6.

$$\text{Glycine} + \text{PlGoxA}(\text{CTQ}_{ox}) \xrightarrow{K_d} \text{Glycine} - \text{PlGoxA}(\text{CTQ}_{ox}) \xrightleftharpoons[k_{-red}]{k_{red}} \text{Glycine} \quad (5)$$

$$- \text{PlGoxA}(\text{CTQ}_{red})$$

$$k_{obs} = k_{red}[\text{Glycine}]/([\text{Glycine}] + K_d) + k_{-red} \quad (6)$$

Size exclusion chromatography

Size exclusion chromatography was performed with an AKTA Prime FPLC system using a HiLoad 16/600 Superdex 200 (GE Healthcare). Chromatography was performed in 50 mM tris-HCl buffer plus 150 mM NaCl at pH 7.5. The flow rate was 0.6 mL/min. The void volume was calculated using blue dextran, the molecular weight markers were apoferritin (442 kDa), glutamate dehydrogenase (332 kDa), amylase (200 kDa), methylamine dehydrogenase (124 kDa), MauG (42.3 kDa) and amicyanin (11.5 kDa). A plot of the elution volume/void volume versus log molecular weight was used to estimate the mass of PlGoxA.

PlGoxA reduction

PlGoxA was anaerobically reduced either by the glycine substrate or by the single-electron reductant, dithionite, in order to visualize the changes to the CTQ spectral feature. Experiments were performed in 50 mM phosphate buffer, pH 7.5, at 25°C. In order to monitor the effects of post-reduction oxidation, air was introduced by removing the cap from the cuvette. Alternately, rapid oxidation was achieved by bubbling O_2 gas into the cuvette after removing the cap.

Crystallization and structure determination

Initial crystallization hits were identified using the Haupton Woodward Institute standard screen [20]. These were optimized in house and diffraction quality crystals were grown under paraffin oil using a 1:1 ratio of 10 mg/mL PlGoxA and precipitant solution containing 0.1 M HEPES pH 7.5, 0.1 M ammonium sulfate and 18– 22% PEG 3350 at 292 K. To generate lead derivatives, crystals were soaked in mother liquor containing 10 mM trimethyl lead acetate for 10 min, followed by backsoaking and cryoprotection in mother liquor containing 10% PEG 400 prior to cryocooling in liquid nitrogen.

Diffraction data were collected at 100 K on beamline 5.0.2 at the Advanced Light Source at Berkeley National Laboratory, indexed and integrated with XDS [21, 22] and scaled using Aimless [23]. A weak molecular replacement (MR) solution was found using MRAGE [24] with an input model based on LodA from *M. mediterranea* (PDB code 3WEU) [25], but the

resulting electron density map failed to yield a structure. This MR solution was combined with single wavelength anomalous dispersion (SAD) data from a lead derivative crystal to generate a solution using Phenix AutoSol [26]. The initial solution was subjected to several rounds of automated model building, density modification and refinement using the Phenix AutoBuild Wizard [27]. Manual model building was done in Coot [28], further rounds of refinement and calculation of anomalous difference maps were performed using the Phenix suite [29]. Atomic coordinates of PlGoxA have been deposited in the PDB with entry code 6BYW. Figures were prepared using Pymol (http://www.pymol.org), which was also used for pairwise structural alignments and calculations of solvent accessible surface area.

RESULTS

Identification and phylogenetic analysis of GoxA-like proteins

The number of available bacterial genomes is increasing due to the improvement and decrease of cost of the sequencing process. The genus *Pseudoalteromonas* is able to synthesize different amino acid oxidases but the genes coding for those enzymes remains in many cases unidentified [16]. The genomes of two *P. luteoviolacea* strains, CPMOR-1 and CPMOR-2, have been recently made available. Genome mining of these two strains revealed in CPMOR-2 a gene encoding a protein with similarity to MmGoxA, which we have named as PlGoxA in this study. The previous phylogenetic study of LodA-like proteins identified 168 proteins that clustered in five different major groups, with MmGoxA in Group II [15]. Since PlGoxA was not included in this analysis and new genomes have been sequenced, a new BLASTP search [30] was performed using MmGoxA as query and a cut-off limit for the E-value of $1e^{-20}$, against the Integrated Microbial Genomes (IMG) database of genome sequences as of July 8, 2017. In this new analysis, 500 genes encoding LodA-like proteins were detected. This indicates a large increase in the number of LodA-like proteins in the database during the past two years. The phylogenetic analysis using the detected proteins showed that Group II, which was previously comprised of 19 proteins, now contains 77 proteins. Genes encoding proteins of Group II are most frequent in *Alphaproteobacteria, Gammabacteria* and *Flavobacteria* (Table 1). The increased number of proteins in this group allowed these proteins to be clearly divided into four well-defined subgroups (Figure S1). Most of proteins in Group IIA and IIB are encoded by genes present in *Alphaproteobacteria*, but it also contains MmGoxA from the gammaproteobacterium *M. mediterranea*, and other genes in the betaproteobacterium *Alcaligenes faecalis* and the cyanobacterium *Synechococcus* sp. 7805. Group IIC contains genes from *Flavobacteria*. The GoxA-like proteins encoded by genes from the microorganisms of the genus *Pseudoalteromonas* reside in Group IID.

Immediately downstream of Pl*goxA* in *P. luteoviolacea* CPMOR-2 there is another gene (Pl*goxB*) whose product exhibits 44.2% sequence similarity with the *goxB* from *M. mediterranea*. Both genes appear to form part of the same operon, as has been demonstrated for LodA and MmGoxA [10, 31] (Figure 2), which are also encoded by operons containing two genes. It cannot be ruled out that the gene upstream that codes for enamine dehydrogenase RidA also forms part of the same operon.

Sequence comparison of PlGoxA and MmGoxA

Alignment of the amino acid sequences of MmGoxA and PlGoxA reveals interesting distinctions and similarities (Figure 3). With 816 amino acid residues, PlGoxA is significantly larger than MmGoxA, which has 678 residues. Another important distinction is that MmGoxA possesses a twin-arginine signal peptide sequence [32] at the N-terminus. On the contrary, PlGoxA lacks this signal sequence. However, analysis of the sequence of PlGoxA using the SecretomeP 2.0 Server (http://www.cbs.dtu.dk/services/SecretomeP) predicted it to be a secreted protein exported by a "non-classical" secretion system [33]. It received a score of 0.937, with 1.0 being the maximum score.

PlGoxA exhibits 39.6% overall sequence similarity to MmGoxA. Despite the differences in sequence discussed above, key residues essential for the activity of MmGoxA are conserved in the alignment of the sequence with PlGoxA. Cys551 and Tpr566, which are modified to form CTQ in MmGoxA, correspond to Cys682 and Trp697 in the PlGoxA sequence. Asp547 of MmGoxA is essential for CTQ generation [14] and is structurally conserved in LodA [25] as well as the CTQ- and TTQ-dependent dehydrogenases [11]. This corresponds to Asp678 in PlGoxA. His466 that is critical for CTQ biogenesis in MmGoxA corresponds to His583 in PlGoxA. Phe237 of MmGoxA, which is involved in cooperativity and homodimer stabilization [11], corresponds to Phe316 in PlGoxA.

Purification and physical properties of PlGoxA

In order to produce PlGoxA with the mature CTQ cofactor, the genes Pl*goxA* and Pl*goxB* were cloned and expressed together in *E. coli*. The yield of the purified PlGoxA protein was approximately 14 mg per g of cells, wet weight. The molecular weight of PlGoxA with the added His-tag is predicted from the sequence to be 92,238 Da, consistent with its position of migration of on SDS-PAGE. When subjected to size-exclusion chromatography, it eluted with an apparent mass of 373 kDa (Figure 4), suggesting that it is a tetramer in solution. This is noteworthy because MmGoxA eluted as a dimer when analyzed in this manner [35].

The crystal structure of PlGoxA

Attempts to solve the crystal structure of PlGoxA using molecular replacement (MR) with the structure of LodA as a search model failed. The structure was solved using a combined MR – single wavelength anomalous dispersion (MR-SAD) approach with SAD data collected on a crystal soaked in trimethyl lead acetate (Table 2). PlGoxA crystallizes as a homotetramer, with four protein chains within the asymmetric unit (Figure 5A). The structure can be thought of as a dimer of dimers. A grooved, head-to-head homodimer is generated by interaction between two chains (Figure 5B), which buries 6,083 Å^2 of solvent accessible surface area (~19% of monomer total). Interaction between the grooves of two homodimers arranged orthogonally to one another buries and interface 8,957 Å^2 (~14% of monomer total per monomer) and generates the homo-tetramer. The large buried surface areas are consistent with size-exclusion chromatography results indicating that PlGoxA exists as a homo-tetramer in solution.

As predicted from sequence alignments, Cys682 and Trp697 of PlGoxA have been post-translationally modified to generate the CTQ cofactor (Figure 5C). It is located in a small

pocket at the base of a deep cleft. The pocket can accommodate several water molecules, but access to it appears to be blocked by a loop from the neighboring monomer comprised of residues 760 -771, which projects into the cleft housing the active site CTQ (Figure 5B). Specifically, the side chains of Tyr766 and His767 project into the entrance to the active site pocket and are stabilized in this position by primarily hydrophobic and π-stacking interactions with Phe316, Tyr772, His583 and Ile507 (Figure 5D). Tyr766 also engages hydrogen bond interactions with His583 and active site waters connecting it to the CTQ cofactor.

Comparison of the structures of PlGoxA and LodA reveals that the striking beta-barrel feature and much of the core alpha helical structure of LodA is conserved in PlGoxA (Figure 6A). Similarly, the positions of residues Asp678 and His583 are conserved with Asp512 and Cys448 of LodA [25] (Figure 6B) where they are essential for cofactor biosynthesis and activity [14, 36]. However, PlGoxA differs from of LodA in other important aspects. PlGoxA lacks the long antiparallel beta-strand "arms" found in LodA that appear to mediate interactions between monomers. The quaternary structure in LodA presents a much larger and more accessible active site than is observed in PlGoxA, where interactions between monomers completely block access to the CTQ cofactor and severely limit the size of the active site pocket. Furthermore, PlGoxA residues 45-140, which are not conserved in either LodA or GoxA, comprise a small alpha helical domain at the periphery of the protein. This segment is conserved only in the proteins of Group IID. Electron density was relatively weak in this region and B-factors were significantly higher than average, which indicates that there is considerable flexibility of this domain as a whole. A search of the DALI server [37] revealed little similarity to known structures, and conserved domain databases failed to identify this sequence.

Steady-state kinetic properties of PlGoxA

Kinetic studies of PlGoxA were performed to characterize its glycine oxidase activity. To determine the steady-state parameters for the glycine oxidase activity of PlGoxA, initially the concentration of the glycine was varied in the presence of room air (252 μM O_2). As it was previously reported that MmGoxA exhibited allosteric cooperativity for its glycine substrate (12), initial rates were measured and the data were fit by both the Michaelis-Menten equation (eq 3) and the Hill equation (eq 4). The fit to the former yielded values of k_{cat}=6.6±0.3 s^{-1} and K_m=219±37 μM with an R^2=0.956. The fit of the data by eq 4 yielded values of k_{cat}=6.0±0.2 s^{-1}, $K_{0.5}$=187±18 μM and h=1.77±0.27 with an improved value of R^2 of 0.990, confirming that PlGoxA exhibits positive cooperativity (Figure 7A). This result for the tetrameric PlGoxA is similar to what was observed for the dimeric MmGoxA which exhibited an h=1.8 (12). When the reaction was studied in the presence of 100% O_2-saturated (1150 μM) buffer the cooperativity was less pronounced. The fit of the data by Eq 4 yields values of k_{cat}=14.7±0.5 s^{-1}, $K_{0.5}$=454±49 μM and h=1.36±0.12 with an R^2 of 0.997 (Figure 7B.). Subsequent studies were performed under room air conditions.

Spectroscopic properties of different forms of PlGoxA

The changes in the visible absorbance spectrum that were observed on reduction of PlGoxA by the glycine substrate and by dithionite were distinct from those observed previously for other CTQ and TTQ enzymes.

Oxidized spectrum—The spectrum of oxidized PlGoxA has a broad absorbance in the 350-450 nm range comprised of two overlapping peaks centered at 365 and 410 nm (Figure 8A, black spectrum). This spectral feature is similar to those exhibited by the other CTQ oxidases LodA and MmGoxA, but distinct from CTQ and TTQ-containing dehydrogenases. The spectrum of the oxidized form of the TTQ-bearing methylamine dehydrogenase (MADH) exhibits a broad peak centered at 440 nm [38]. For the CTQ-dependent QHNDH it was not possible to observe the CTQ absorbance features in the holoenzyme as they are masked by the presence of the hemes. For the isolated CTQ-bearing subunit, which was separated from the heme-bearing subunit of the trimeric QHNDH, the oxidized state exhibits a broad peak centered at 380 nm rather than overlapping peaks [39]. Thus, the two overlapping peaks rather than a single peak in this region of the spectrum seems to be specific for the CTQ-dependent oxidases.

Glycine-reduced spectrum—Anaerobic addition of glycine to PlGoxA generates a complex spectrum (Figure 8A). The features of the oxidized protein are bleached and two new broad peaks are formed which are centered at 440 and 600 nm. In fact, because of the 600 nm absorbance the solution turns visibly blue. Formation of a shoulder off the 280 peak extending to 340 nm is also observed. The appearance of the new peaks at higher wavelength is unique to PlGoxA. The CTQ-bearing subunit of QHNDH could not be reduced by substrate, as it is inactive when separated from the other subunits. However, full reduction of CTQ in the subunit by dithionite caused bleaching of the peak at 440 nm and appearance of a small shoulder off the 280 nm absorbance at approximately 315 nm [39], but no absorbance at higher wavelengths. Full reduction of the TTQ enzyme MADH by either dithionite or methylamine caused bleaching of the peak at 440 nm and formation of a large sharp peak at 330 nm [38], but no peaks at higher wavelengths. When the glycine-reduced PlGoxA was exposed to air by simply removing the cap on the cuvette, the spectrum slowly returned to that of the oxidized form (Figure 8B). No intermediated spectroscopic states were observed during the oxidation. Alternatively, when the glycine-reduced PlGoxA was briefly bubbled with 100% O_2, the return to the oxidized spectrum was immediate.

Dithionite-reduced spectrum—Another interesting feature of PlGoxA is that addition of excess dithionite to the oxidized protein yielded a spectral change different from that observed on addition of glycine. PlGoxA could not be stoichiometrically reduced with dithionite. Addition of 200 μM dithionite (10-fold excess of protein concentration) to oxidized PlGoxA was required to observe this change, which was complete after 400 s. In the resulting spectrum (Figure 9) the oxidized peaks were bleached, as was seen with the glycine-reduced PlGoxA. However, the appearance of peaks at 440 nm and 600 nm was not observed. The lower wavelength region of the spectrum was unfortunately obscured because of the absorbance of the excess dithionite required for reduction. However, the most prominent feature of the dithionite-reduced spectrum is a new sharp peak at 380 nm, which

was not observed in the substrate-reduced spectrum. This spectral feature is reminiscent of the semiquinone form of TTQ in MADH that could be generated by addition of one-electron equivalent of dithionite to the enzyme, and exhibits a sharp peak at 428 nm [38]. This suggests that dithionite primarily reduces PlGoxA to the semiquinone state. Addition of up to 1.0 mM dithionite produced no further spectral change. On exposure of this dithionite-reduced form of the enzyme to air or 100 % O_2, the spectrum returned to that of the oxidized form (Figure 9).

Kinetic isotope effect study of the reduction of PlGoxA by glycine

It was previously observed that the TTQ-dependent enzymes MADH and AADH each exhibited anomalously large deuterium kinetic isotope effect (KIE) of 17.2 [40] and 11.7 [41], respectively, on the rate of reduction of TTQ by substrate in single-turnover kinetics studies. These values suggested a mechanism for the reductive half-reaction in which TTQ reduction is linked to proton abstraction from a covalent enzyme-substrate intermediate, and that this was a rate-determining proton tunneling event. As such, analogous single-turnover kinetic studies of the reduction of CTQ were performed using glycine with PlGoxA. Analysis of the rate of reduction (k_{red}) of CTQ at varied concentrations of glycine by Eq 6 yielded a k_{red} of 9.3 ± 1.3 s^{-1} and a K_d of 565 ± 348 μM (Figure 10). To determine whether k_{red} in PlGoxA also exhibits a primary KIE, reactions were performed in room air an initiated by addition of 5 mM glycine or glycine-d$_5$. This concentration was well above the $K_{0.5}$ to ensure that any observed KIE would not be influenced by substrate binding events. The reaction with PlGoxA did not exhibit a significant primary KIE. The values of k_{red} for glycine and glycine-d$_5$ were 9.8 ± 0.2 s^{-1} and 9.1 ± 0.2 s^{-1}, yielding a KIE of 1.08 ± 0.03.

DISCUSSION

The structure, kinetic properties and spectroscopic properties of PlGoxA are each distinct from those of other quinoproteins as well as from other glycine oxidases. Traditional glycine oxidases (EC 1.4.3.19) contain non-covalently bound FAD. They have been previously described in microorganisms of the genera *Bacillus* [42-44], *Geobacillus* [45] and *Pseudomonas* [46]. Glycine oxidase from *B. subtilis* (ThiO) participates in the biosynthesis of the thiazole moiety of the thiamin [47]. This class of enzymes has been used for a variety of applications such as the design of biosensors, agricultural biotechnology and industrial biocatalysis [48-50]. These glycine oxidases show similarity in sequence and substrate range with other flavoenzymes, D-amino acid oxidases (EC 1.4.3.3) and sarcosine oxidases (EC 1.5.3.1). PlGoxA differs from traditional glycine oxidases as it is much more specific for Gly and it does not utilize FAD, but instead contains CTQ. In fact, phylogenetic analyses have revealed that, in spite of possessing amino acid oxidase activity, the LodA like proteins are in an evolutionary branch separated from the amino acid oxidases with flavin cofactors [12].

The phylogenetic analysis in this study suggests that *goxA*-like genes encoding proteins that cluster in subgroups IIA and IIB have a common ancestor in alphaproteobacteria, while those in subgroup IIC come from flavobacteria and those in group IID are from gammaproteobacteria of the genus *Pseudoalteromonas*. Thus, the GoxA-like proteins in the distinct subgroups have different evolutionary origins, raising interesting questions about the

evolutionary mechanisms and physiological relevance of these proteins. The fact that MmGoxA (subgroup IIB) and PlGoxA (subgroup IID) each exhibit glycine oxidase activity suggests that all of the proteins in the Group II of LodA-like proteins have glycine oxidase activity. In contrast, the proteins in Group I, which includes LodA, are likely all lysine epsilon-oxidases. This was shown for the proteins synthesized by *M. mediterranea* and *Pseudoalteromonas tunicata* [51]. Thus, this work supports the idea that the different phylogenetic groups of LodA-like proteins are related to the activity and substrate specificity of the enzymes belonging to those clusters [15]. As such, it will be interesting to determine the activities of the LodA-like proteins in Groups III-V.

PlGoxA, as well as the other LodA-like proteins described thus far, are distinct from previously described quinoproteins as they possess tryptophylquinone cofactors and function as oxidases rather than dehydrogenases. They are also the first quinoproteins shown to function as amino acid oxidases. The structure of PlGoxA characterized in this study further distinguishes this enzyme from the other previously characterized LodA-like proteins. PlGoxA contains an additional N-terminal domain with no close structural homologues in the PDB and the sequence of which is only conserved among the other Group IID proteins, and completely absent in all other Group II LodA-like sequences. The function of this domain is currently unknown. The quaternary structure of PlGoxA is completely different from that of LodA. The active site is quite small, due to intersubunit interactions involving Tyr766 and His767 from one monomer and His583, Phe316, Tyr772 and Ile507 from another monomer. Interestingly, all of these residues are conserved in MmGoxA (Figure 4), where Phe237 (Phe316 in PlGoxA) was also shown to be important for enzymatic cooperativity and dimer stabilization. It seems likely that Tyr766 and His767 not only limit the size of the active site pocket, but also may interact directly with bound Gly. This interaction would explain both the cooperative activity of GoxA as well as its strict specificity for Gly, as other amino acids would be too large to interact optimally. The similar Hill coefficients obtained for the dimeric MmGoxA and the tetrameric PlGoxA suggest that PlGoxA may function catalytically more like a dimer of cooperative dimers than a cooperative homo-tetramer.

The spectroscopic descriptions of the different redox forms of PlGoxA are also notable. The two overlapping peaks at 365 and 410 nm rather than a single peak in this region of the oxidized PlGoxA spectrum seems to be specific for the CTQ-dependent oxidases. The spectra of the TTQ-bearing dehydrogenases [38] and CTQ-bearing subunit of QHNDH [39] each exhibit a single broad peak centered at 440 and 380 nm, respectively, rather than overlapping peaks. The appearance of stable absorbance features at higher wavelengths (400 and 600 nm) after reduction by substrate is unique to PlGoxA and has not been reported for any other TTQ- or CTQ-dependent enzyme. Full reduction of the TTQ enzyme MADH by either dithionite or methylamine caused bleaching of the peak at 440 nm and formation of a large sharp peak at 330 nm assigned to the quinol form. A very similar spectrum was obtained for the reduced aminoquinol form of the enzyme[52], which is the intermediate present after hydrolysis to release the aldehyde product from the TTQ-product adduct after reaction. Thus, it is unlikely that the unusual spectral features of the substrate-reduced PlGoxA can be attributed to the aminoquinol form of CTQ. It is possible that these absorbance features may be attributed to the glycine-CTQ adduct after CTQ reduction prior to hydrolysis, which then

occurs concomitant with the reaction with O_2. Alternatively, it may be related to the environment surrounding either the Cys or tryptophylquinone portion of the cofactor.

The spectrum of PlGoxA in the presence of excess dithionite is similar to that of the semiquinone form of TTQ in MADH generated by addition of one-electron equivalent of dithionite to the enzyme and exhibiting a sharp peak at 428 nm[38]. However, the TTQ semiquinone could be further reduced to the quinol, albeit much more slowly, while PlGoxA remains in the semiquinone state even with excess dithionite. Given the reducing power of dithionite, this suggests that there is a kinetic rather than a thermodynamic barrier to the reduction of the semiquinone in each case and that the barrier to full reduction is more extreme in PlGoxA than MADH. It is possible that the conversion of the CTQ quinone to the semiquinone may be accompanied by a change in conformation that makes the cofactor less accessible to dithionite for further reduction.

The kinetic data obtained in this study suggest that the kinetic mechanism of PlGox may be unique among quinoprotein dehydrogenases and oxidases. For the TTQ-dependent amine dehydrogenases, the rate-determining step in the overall reaction is the proton transfer from the substrate-TTQ adduct which occurs concomitant with TTQ reduction. This step involves proton tunneling. Furthermore, hydrolysis of the reduced adduct to release the aldehyde product occurs immediately afterwards, prior to re-oxidation, yielding an aminoquinol intermediate. For PlGoxA no primary KIE is observed in for the reduction step. Furthermore, the formation of a stable substrate-reduced is CTQ adduct is suggested by the unique absorbance spectrum of this species. There are quinoprotein amine oxidases, which do not use a tryptophylquinone cofactor but instead use TPQ in which two oxygen atoms are inserted into a Tyr residue [4, 5]. The reductive half-reaction of these enzymes is essentially identical to that of the TTQ-dependent amine dehydrogenases, and as with the TTQ enzymes, release of the aldehyde product occurs immediately after reduction and prior to re-oxidation, yielding an aminoquinol intermediate [53]. Single-turnover studies of the reduction of TPQ by the amine substrate in bovine serum amine oxidase also showed that this reaction exhibits an anomalously large primary KIE indicative of proton tunneling [54]. Thus, the kinetic and reaction mechanisms of the reductive half-reaction of PlGoxA appear to be distinct from both those of TTQ-dependent amine dehydrogenases and TPQ-dependent amine oxidases. Future characterization of the structures of reaction intermediates of PlGoxA and more detailed mechanistic studies should expand our view of possible mechanisms of catalysis by quinone cofactors.

Supplementary Material

Refer to Web version on PubMed Central for supplementary material.

Acknowledgments

ABBREVIATIONS

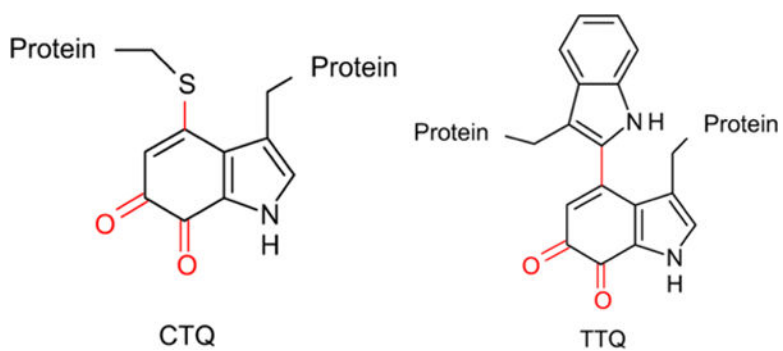|	
CTQ	cysteine tryptophylquinone
KIE	kinetic isotope effect
MADH	methylamine dehydrogenase
MR	molecular replacement
QHNDH	quinohemoproteine amine dehydrogenase
SAD	single wavelength anomalous dispersion
TPQ	topaquinone
TTQ	tryptophan tryptophylquinone
WT	wild-type

References

1. Davidson VL. Pyrroloquinoline quinone (PQQ) from methanol dehydrogenase and tryptophan tryptophylquinone (TTQ) from methylamine dehydrogenase. Adv Protein Chem. 2001; 58:95–140. [PubMed: 11665494]

2. Davidson VL. Protein-derived cofactors. Expanding the scope of post-translational modifications. Biochemistry. 2007; 46:5283–5292. [PubMed: 17439161]

3. Davidson VL. Generation of protein-derived redox cofactors by posttranslational modification. Mol Biosyst. 2011; 7:29–37. [PubMed: 20936199]

4. Janes SM, Mu D, Wemmer D, Smith AJ, Kaur S, Maltby D, Burlingame AL, Klinman JP. A new redox cofactor in eukaryotic enzymes: 6-hydroxydopa at the active site of bovine serum amine oxidase. Science. 1990; 248:981–987. [PubMed: 2111581]

5. Mure M. Tyrosine-derived quinone cofactors. Acc Chem Res. 2004; 37:131–139. [PubMed: 14967060]

6. Wang SX, Mure M, Medzihradszky KF, Burlingame AL, Brown DE, Dooley DM, Smith AJ, Kagan HM, Klinman JP. A crosslinked cofactor in lysyl oxidase: redox function for amino acid side chains. Science. 1996; 273:1078–1084. [PubMed: 8688089]

7. McIntire WS, Wemmer DE, Chistoserdov A, Lidstrom ME. A new cofactor in a prokaryotic enzyme: tryptophan tryptophylquinone as the redox prosthetic group in methylamine dehydrogenase. Science. 1991; 252:817–824. [PubMed: 2028257]

8. Datta S, Mori Y, Takagi K, Kawaguchi K, Chen ZW, Okajima T, Kuroda S, Ikeda T, Kano K, Tanizawa K, Mathews FS. Structure of a quinohemoprotein amine dehydrogenase with an uncommon redox cofactor and highly unusual crosslinking. Proc Natl Acad Sci U S A. 2001; 98:14268–14273. [PubMed: 11717396]

9. Gomez D, Lucas-Elio P, Sanchez-Amat A, Solano F. A novel type of lysine oxidase: L-lysine-epsilon-oxidase. Biochim Biophys Acta. 2006; 1764:1577–1585. [PubMed: 17030025]

10. Campillo-Brocal JC, Lucas-El¡o P, Snchez-Amat A. Identification in *Marinomonas mediterranea* of a novel quinoprotein with glycine oxidase activity. Microbiologyopen. 2013; 2:684–694. [PubMed: 23873697]

11. Sehanobish E, Williamson HR, Davidson VL. Roles of conserved residues of the glycine oxidase GoxA in controlling activity, cooperativity, subunit composition, and cysteine tryptophylquinone biosynthesis. J Biol Chem. 2016; 291:23199–23207. [PubMed: 27637328]

12. Campillo-Brocal JC, Lucas-Elio P, Sanchez-Amat A. Distribution in different organisms of amino acid oxidases with FAD or a quinone as cofactor and their role as antimicrobial proteins in marine bacteria. Mar Drugs. 2015; 13:7403–7418. [PubMed: 26694422]

13. Gomez D, Lucas-Elio P, Solano F, Sanchez-Amat A. Both genes in the *Marinomonas mediterranea* lodAB operon are required for the expression of the antimicrobial protein lysine oxidase. Mol Microbiol. 2010; 75:462–473. [PubMed: 20025674]

14. Chacon-Verdu MD, Campillo-Brocal JC, Lucas-Elio P, Davidson VL, Sanchez-Amat A. Characterization of recombinant biosynthetic precursors of the cysteine tryptophylquinone cofactors of l-lysine-epsilon-oxidase and glycine oxidase from Marinomonas mediterranea. Biochim Biophys Acta. 2015; 1854:1123–1131. [PubMed: 25542375]

15. Campillo-Brocal JC, Chacon-Verdu MD, Lucas-El¡o P, Snchez-Amat A. Distribution in microbial genomes of genes similar to *lodA* and *goxA* which encode a novel family of quinoproteins with amino acid oxidase activity. BMC.Genomics. 2015; 16:231. [PubMed: 25886995]

16. Gomez D, Espinosa E, Bertazzo M, Lucas-Elio P, Solano F, Sanchez-Amat A. The macromolecule with antimicrobial activity synthesized by *Pseudoalteromonas luteoviolacea* strains is an L-amino acid oxidase. Appl Microbiol Biotechnol. 2008; 79:925–930. [PubMed: 18504575]

17. Chen IA, Markowitz VM, Chu K, Palaniappan K, Szeto E, Pillay M, Ratner A, Huang J, Andersen E, Huntemann M, Varghese N, Hadjithomas M, Tennessen K, Nielsen T, Ivanova NN, Kyrpides NC. IMG/M: integrated genome and metagenome comparative data analysis system. Nucleic Acids Res. 2017; 45:D507–D516. [PubMed: 27738135]

18. Edgar RC. MUSCLE: multiple sequence alignment with high accuracy and high throughput. Nucleic Acids Res. 2004; 32:1792–1797. [PubMed: 15034147]

19. Tamura K, Stecher G, Peterson D, Filipski A, Kumar S. MEGA6: Molecular Evolutionary Genetics Analysis version 6.0. Mol Biol Evol. 2013; 30:2725–2729. [PubMed: 24132122]

20. Luft JR, Collins RJ, Fehrman NA, Lauricella AM, Veatch CK, DeTitta GT. A deliberate approach to screening for initial crystallization conditions of biological *macromolecules*. J Struct Biol. 2003; 142:170–179. [PubMed: 12718929]

21. Kabsch W. Xds, Acta Crystallogr D Biol Crystallogr. 2010; 66:125–132. [PubMed: 20124692]

22. Kabsch W. Integration, scaling, space-group assignment and post-refinement. Acta Crystallogr D Biol Crystallogr. 2010; 66:133–144. [PubMed: 20124693]

23. Winn MD, Ballard CC, Cowtan KD, Dodson EJ, Emsley P, Evans PR, Keegan RM, Krissinel EB, Leslie AG, McCoy A, McNicholas SJ, Murshudov GN, Pannu NS, Potterton EA, Powell HR, Read RJ, Vagin A, Wilson KS. Overview of the CCP4 suite and current developments. Acta Crystallogr D Biol Crystallogr. 2011; 67:235–242. [PubMed: 21460441]

24. Bunkoczi G, Echols N, McCoy AJ, Oeffner RD, Adams PD, Read RJ. Phaser.MRage: automated molecular replacement. Acta Crystallogr D Biol Crystallogr. 2013; 69:2276–2286. [PubMed: 24189240]

25. Okazaki S, Nakano S, Matsui D, Akaji S, Inagaki K, Asano Y. X-Ray crystallographic evidence for the presence of the cysteine tryptophylquinone cofactor in L-lysine epsilon-oxidase from *Marinomonas mediterranea*. J Biochem. 2013; 154:233–236. [PubMed: 23908359]

26. Terwilliger TC, Grosse-Kunstleve RW, Afonine PV, Moriarty NW, Zwart PH, Hung LW, Read RJ, Adams PD. Iterative model building, structure refinement and density modification with the PHENIX AutoBuild wizard. Acta Crystallogr D Biol Crystallogr. 2008; 64:61–69. [PubMed: 18094468]

27. Terwilliger TC, Adams PD, Read RJ, McCoy AJ, Moriarty NW, Grosse-Kunstleve RW, Afonine PV, Zwart PH, Hung LW. Decision-making in structure solution using Bayesian estimates of map quality: the PHENIX AutoSol wizard. Acta Crystallogr D Biol Crystallogr. 2009; 65:582–601. [PubMed: 19465773]

28. Emsley P, Cowtan K. Coot: model-building tools for molecular graphics. Acta Crystallogr D Biol Crystallogr. 2004; 60:2126–2132. [PubMed: 15572765]

29. Adams PD, Afonine PV, Bunkoczi G, Chen VB, Davis IW, Echols N, Headd JJ, Hung LW, Kapral GJ, Grosse-Kunstleve RW, McCoy AJ, Moriarty NW, Oeffner R, Read RJ, Richardson DC, Richardson JS, Terwilliger TC, Zwart PH. PHENIX: a comprehensive Python-based system for macromolecular structure solution. Acta Crystallogr D Biol Crystallogr. 2010; 66:213–221. [PubMed: 20124702]

30. Boratyn GM, Camacho C, Cooper PS, Coulouris G, Fong A, Ma N, Madden TL, Matten WT, McGinnis SD, Merezhuk Y, Raytselis Y, Sayers EW, Tao T, Ye J, Zaretskaya I. BLAST: a more
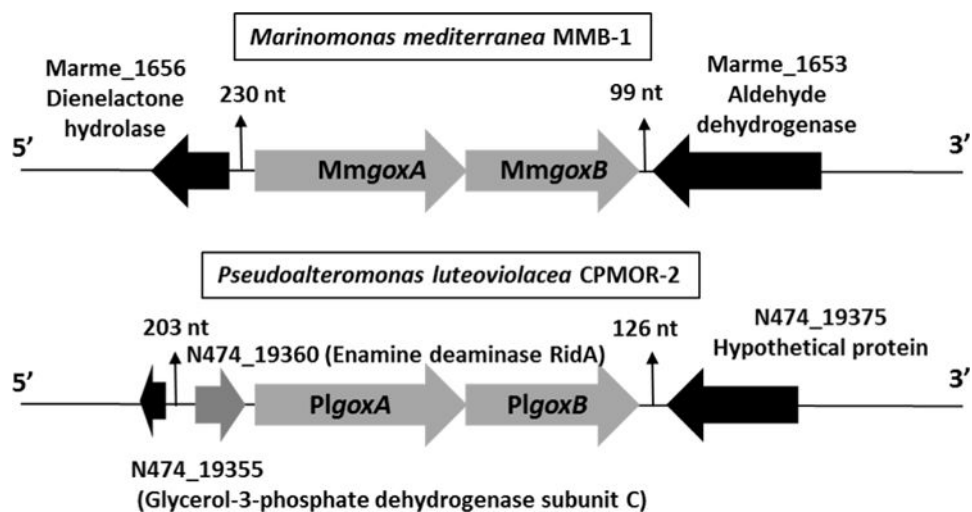
efficient report with usability improvements. Nucleic Acids Res. 2013; 41:W29–W33. [PubMed: 23609542]

31. Lucas-Elio P, Gomez D, Solano F, Sanchez-Amat A. The antimicrobial activity of marinocine, synthesized by *Marinomonas mediterranea*, is due to hydrogen peroxide generated by its lysine oxidase activity. J Bacteriol. 2006; 188:2493–2501. [PubMed: 16547036]

32. Bendtsen JD, Nielsen H, Widdick D, Palmer T, Brunak S. Prediction of twin-arginine signal peptides. BMC.Bioinformatics. 2005; 6:167. [PubMed: 15992409]

33. Bendtsen JD, Kiemer L, Fausboll A, Brunak S. Non-classical protein secretion in bacteria. BMC Microbiol. 2005; 5:58. [PubMed: 16212653]

34. Sievers F, Wilm A, Dineen D, Gibson TJ, Karplus K, Li W, Lopez R, McWilliam H, Remmert M, Soding J, Thompson JD, Higgins DG. Fast, scalable generation of high-quality protein multiple sequence alignments using Clustal Omega. Mol Syst Biol. 2011; 7:539. [PubMed: 21988835]

35. Sehanobish E, Campillo-Brocal JC, Williamson HR, Sanchez-Amat A, Davidson VL. Interaction of GoxA with its modifying enzyme and its subunit assembly are dependent on the extent of cysteine tryptophylquinone biosynthesis. Biochemistry. 2016; 55:2305–2308. [PubMed: 27064961]

36. Sehanobish E, Chacon-Verdu MD, Sanchez-Amat A, Davidson VL. Roles of active site residues in LodA, a cysteine tryptophylquinone dependent epsilon-lysine oxidase. Arch Biochem Biophys. 2015; 579:26–32. [PubMed: 26048732]

37. Holm L, Rosenstrom P. Dali server: conservation mapping in 3D. Nucleic Acids Res. 2010; 38:W545–549. [PubMed: 20457744]

38. Husain M, Davidson VL, Gray KA, Knaff DB. Redox properties of the quinoprotein methylamine dehydrogenase from *Paracoccus denitrificans*. Biochemistry. 1987; 26:4139–4143. [PubMed: 3651442]

39. Fujieda N, Mori M, Kano K, Ikeda T. Spectroelectrochemical evaluation of redox potentials of cysteine tryptophylquinone and two hemes c in quinohemoprotein amine dehydrogenase from *Paracoccus denitrificans*. Biochemistry. 2002; 41:13736–13743. [PubMed: 12427036]

40. Brooks HB, Jones LH, Davidson VL. Deuterium kinetic isotope effect and stopped-flow kinetic studies of the quinoprotein methylamine dehydrogenase. Biochemistry. 1993; 32:2725–2729. [PubMed: 8448129]

41. Hyun YL, Davidson VL. Unusually large isotope effect for the reaction of aromatic amine dehydrogenase. A common feature of quinoproteins? Biochim Biophys Acta. 1995; 1251:198–200. [PubMed: 7669810]

42. Nishiya Y, Imanaka T. Purification and characterization of a novel glycine oxidase from *Bacillus subtilis*. FEBS Letters. 1998; 438:263–166. [PubMed: 9827558]

43. Zhan T, Zhang K, Chen Y, Lin Y, Wu G, Zhang L, Yao P, Shao Z, Liu Z. Improving glyphosate oxidation activity of glycine oxidase from *Bacillus cereus* by directed evolution. PLoS ONE. 2013; 8:e79175. [PubMed: 24223901]

44. Zhang K, Guo Y, Yao P, Lin Y, Kumar A, Liu Z, Wu G, Zhang L. Characterization and directed evolution of BliGO, a novel glycine oxidase from *Bacillus licheniformis*. Enzyme Microb Technol. 2016; 85:12–18. [PubMed: 26920475]

45. Martinez-Martinez I, Navarro-Fernandez J, Garcia-Carmona F, Takami H, Sanchez-Ferrer A. Characterization and structural modeling of a novel thermostable glycine oxidase from *Geobacillus kaustophilus* HTA426. Proteins. 2008; 70:1429–1441. [PubMed: 17894345]

46. Equar MY, Tani Y, Mihara H. Purification and Properties of Glycine Oxidase from *Pseudomonas putida* KT2440. J Nutr Sci Vitaminol. 2015; 61:506–510. [PubMed: 26875494]

47. Settembre EC, Dorrestein PC, Park JH, Augustine AM, Begley TP, Ealick SE. Structural and mechanistic studies on ThiO, a glycine oxidase essential for thiamin biosynthesis in *Bacillus subtilis*. Biochemistry. 2003; 42:2971–2981. [PubMed: 12627963]

48. Nicolia A, Ferradini N, Molla G, Biagetti E, Pollegioni L, Veronesi F, Rosellini D. Expression of an evolved engineered variant of a bacterial glycine oxidase leads to glyphosate resistance in alfalfa. J Biotechnol. 2014; 184:201–208. [PubMed: 24905148]

49. Pollegioni L, Molla G. New biotech applications from evolved D-amino acid oxidases. Trends Biotechnol. 2011; 29:276–283. [PubMed: 21397351]

50. Rosini E, Piubelli L, Molla G, Frattini L, Valentino M, Varriale A, D'Auria S, Pollegioni L. Novel biosensors based on optimized glycine oxidase. FEBS Journal. 2014; 281:3460–3472. [PubMed: 24925096]

51. Mai-Prochnow A, Lucas-Elio P, Egan S, Thomas T, Webb JS, Sanchez-Amat A, Kjelleberg S. Hydrogen peroxide linked to lysine oxidase activity facilitates biofilm differentiation and dispersal in several gram-negative bacteria. J Bacteriol. 2008; 190:5493–5501. [PubMed: 18502869]

52. Davidson VL, Brooks HB, Graichen ME, Jones LH, Hyun YL. Detection of intermediates in tryptophan tryptophylquinone enzymes. Methods Enzymol. 1995; 258:176–190. [PubMed: 8524149]

53. Mure M, Mills SA, Klinman JP. Catalytic mechanism of the topa quinone containing copper amine oxidases. Biochemistry. 2002; 41:9269–9278. [PubMed: 12135347]

54. Grant KL, Klinman JP. Evidence that both protium and deuterium undergo significant tunneling in the reaction catalyzed by bovine serum amine oxidase. Biochemistry. 1989; 28:6597–6605. [PubMed: 2790014]
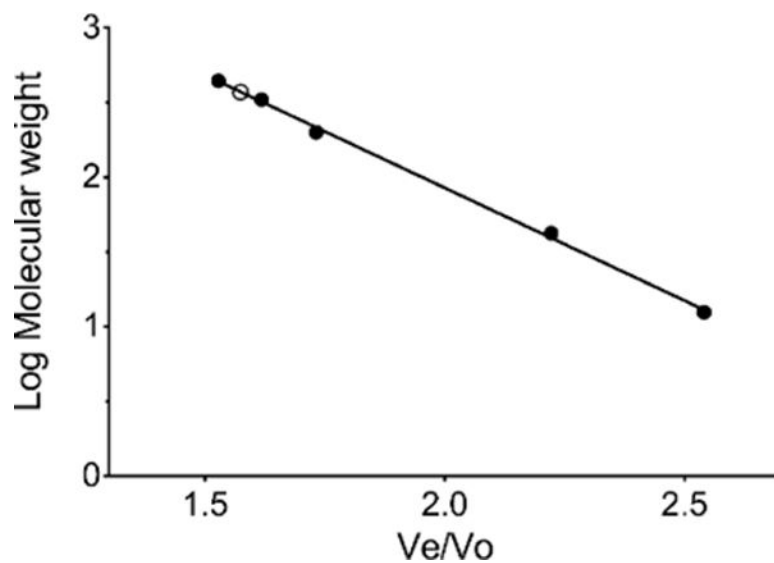
Figure 1.
Protein-derive tryptophylquinone cofactors. Cysteine tryptophylquinone (CTQ) Tryptophan tryptophylquinone (TTQ).
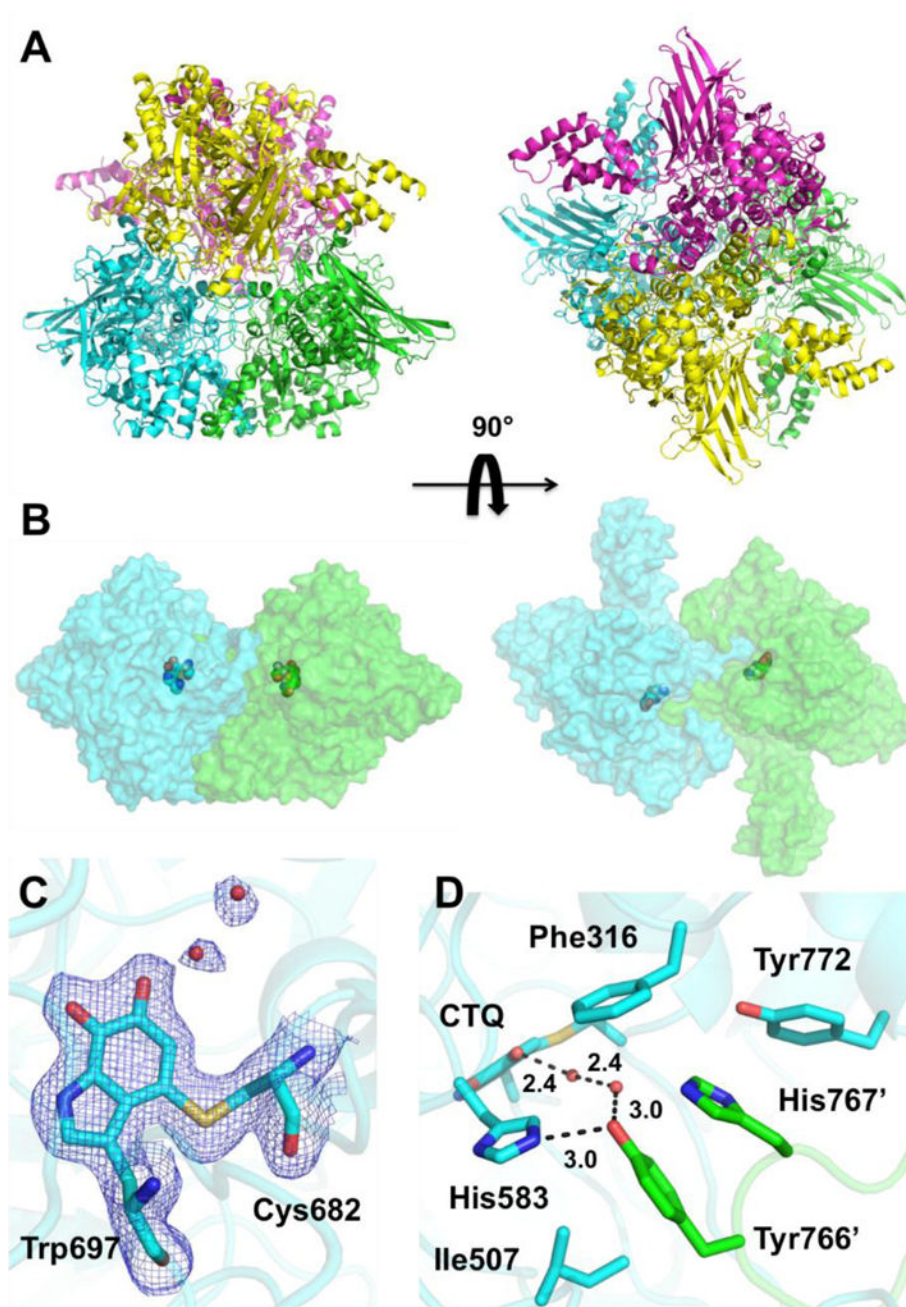
Figure 2.
Genome region around the *goxA* genes in *Marinomonas mediterranea* MMB-1 and *Pseudoalteromonas luteoviolacea* CPMOR-2.

```
PlGoxA    --------------------------------------------------MSNCQYKIYPPL      12
MmGoxA    MQNDGKKMKRRDFLSMAGSVTALS--AFPLIPKSAIA-STHREEAPKDAKIHRLGIYPTI      57
                                                                   *
PlGoxA    GIARVGNGPAIKPLSLSTPEVPWAHLYDTNVQYLVTQQELEQLLEEAFGGNVINEISQIK      72
MmGoxA    GICRVGGSDQYF----LAPEV---------------------------------------      74
          *   *  *            **
PlGoxA    TKLDERKAEKFKQEEIETITGLLGLSHLVPQQQLSRSLDNLELKSTKDSDDIVQQIKGAL     132
MmGoxA    ------------------------------------------------PGLPPMPEGG-      84

PlGoxA    LKVLSDHYLHAVKKQAQNFYIYKCDEQGNPVEKLKLTDGDKVTWRVEVANKKSFWYDYNN     192
MmGoxA    ----FKDGTQAIKKQAQRFRIYAFDDQDRVIGEITE-HNATIEWNVHLANTKAAWYGFNN     139
              ***  * *                      *    * *  **    *
PlGoxA    ALDLSLHTQGSGNLSKNVSKHRLAPAMTAKRRNPNVITNSLRKQLVISSQGSVSSDNNTQ     252
MmGoxA    PLDNGEL---------------APGIPGQKRNQYFVSDEERERMLVINGGERSISGINQ     183
            *                          **
PlGoxA    VPLRGKFPANEPDTNNRLSDLLNLQERHNVLQGSIECDNEGVLRFYAGNGISQALSPSSL     312
MmGoxA    ---------NGDTENDTYQFVGQFWNEETVKLGKIKTDEHGRLIVIPPDGVSNSPT-NAA     233
                             *           * *         *
PlGoxA    NTDFADNSNWFDDICDGRVTAVVELKNGDTFEIQDEQSSAWVATTPPDYAPQIEPIVTMY     372
MmGoxA    ITSFADNDGWHDDWCDGPVQATVKLPDGTFME----ADTAWVACIGPNFAPEIPPVTTLY     289
             *   *  * **  ** *              *         **    *
PlGoxA    DMVSGAALKEQDL---DNLTTQFSDVFPILYRLYRMQWVNQADFTDNAVNTQIRELNSEL     429
MmGoxA    DVISNMNAEQGWTPPVQAPISFRKHIYPIFRRLGLMEWVSSAANLRQG-WLGVGNFSDPA     348
                                *          * *
PlGoxA    GFAQLLDNSASAKSLREGIFNQFRNPLFDQDIDVDDPGQSSNEWVSNSRIIPSKDETNIA     489
MmGoxA    YIKQLADPSPANQAFRQDIFTKFRNPNNVSDTA---------------------------     381
                            *         * *
PlGoxA    AKPATSSLKLPFYPNDGIDYPGSPVQWFAIPPFMYQHLQNWAAGDFSVTQVEKE--SANT     547
MmGoxA    --YLDERLKMPMMLGDGINYDGSPLQWFQFPHQQYQFLEYWAAGNFTNDFEDDKADAIHT     439
                         *    **     **              *     *
PlGoxA    IEELGLFYSEQFKNSPNSALLCARGALDALYGGGFHPGVELTWPMRHNLIYSQNDYVSSV     607
MmGoxA    IEDVDLKLQ------P---DALTEAALEPCSGGAFHPGVELTYYLRIPSMYARNYDNAA-     489
                            **      ** ** ******     *
PlGoxA    TPEINLLGLREFRLKQDLQGLNSPNMYQDFGHVIAVDNVTASIDPNSDAAWLWRSTPGDL     667
MmGoxA    ---------DPFRLA----HRKRDKLVQNIGRLLTLEKAEKGDPALGTSPPLAHQWAGDL     536
                                                                     **
PlGoxA    TKWMGIPWQSDAASCQAVYTPEDFPIPSWWAANLPVHVLPLARYNKFKDSQSADLPEING     727
MmGoxA    TRWMGLPWQCDAFSCQQVLMQEDFPTAVWWPALLPIDVLPEENYTQLMDESLD-------     589
          * ***  ***  *    **  *        ** *  **     **
PlGoxA    MTHSIAQGMSEETFEHLRLEQFSQRLDWLHTADLGFVGYHAEGGYTNGLIQMVSQWKNMA     787
MmGoxA    --------------DSERVKFYENRADWKR--GVAGIGYHANASYWDGITNMITLWERMG     633
                            *  *           * *           *         *
PlGoxA    MVMARPVENPGS----SGIPNVVYVAYSQADKD--------------               816
MmGoxA    FVVKRKGPKGAGTGGLSAVPKEMYVEVGRGNVEDRFKWNPSMGDLPN              680
```

Figure 3.
Protein sequence alignment of MmGoxA and PlGoxA. The alignment was built with Clustal Omeg [34]. Residues conserved in all LodA-like proteins of Group II are designated by *. The Cys and Trp residues that form CTQ are in red. The Asp and His critical for CTQ biogenesis, and Phe involved in cooperativity in MmGoxA are in green. The twin-arginine signal sequence of MmGoxA is underlined with the pair of Arg residues in purple.
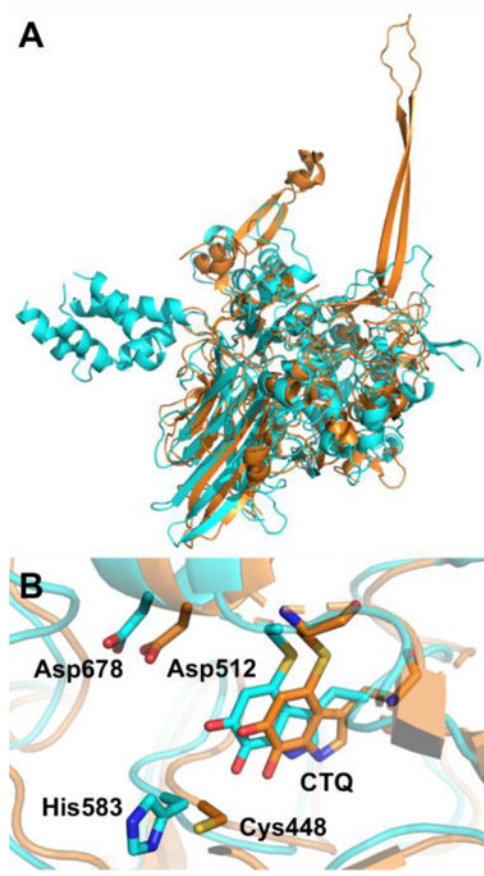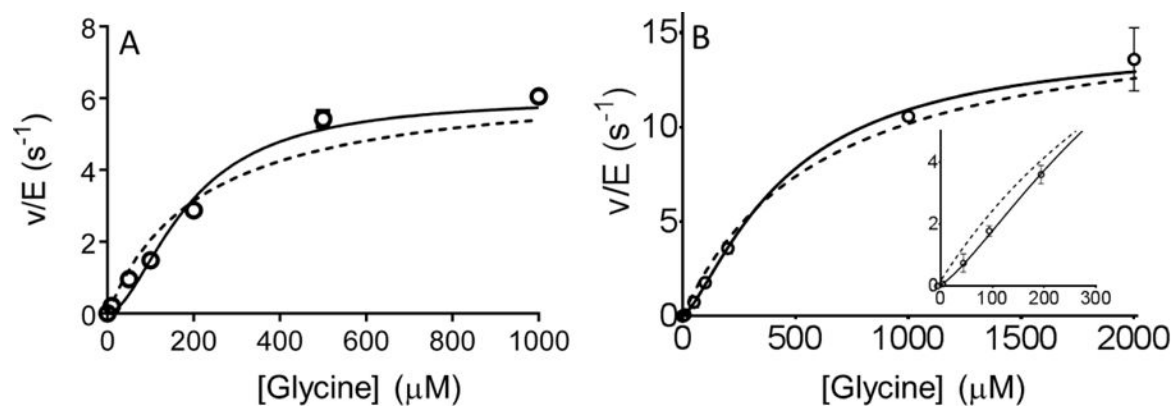
Figure 4.
Size exclusion chromatography. The positions of elution of molecular weight markers are indicated (●): apoferritin (443 kDa) glutamate dehydrogenase (332 kDa), amylase (200 kDa), ethylamine dehydrogenase (124 kDa), MauG (42.3 kDa) and amicyanin (11.5 kDa). The position of elution of GoxA is indicated (o).
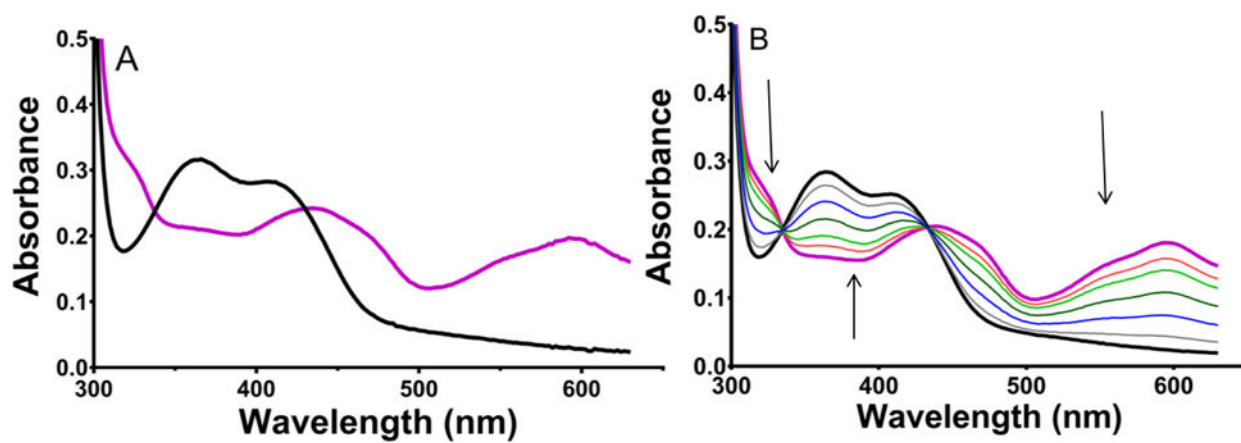
Figure 5.
Structure of PlGoxA. (A) The PlGoxA homo-tetramer is colored by chain presented in cartoon form. (B) One homo-dimer within the homo-tetramer is shown as a transparent surface rendering with the CTQ cofactor depicted as spheres. The colors and orientation are the same as for A. (C) The CTQ cofactor and active site waters are shown with the 2Fo-Fc electron density as blue mesh contoured to 1.0 σ. (D) Interactions between subunits near the active site are shown. Colors are the same are for (A). Dotted lines represent hydrogen bond interactions at the indicated distances in Å.

Figure 6.
Comparison of the structures of PlGoxA and LodA. (A) The structures of monomers of PlGoxA (cyan) and LodA (orange, PDB ID: 3WEU [25]) are displayed in cartoon form and superimposed. (B) The active sites of PlGoxA and LodA are superimposed.

Figure 7.
Steady-state kinetics of the glycine oxidase activity of PlGoxA. (A) Reactions were performed in room air (252 μM). (B) Reactions were performed in 100% O_2 (1150 μM) saturated buffer. (Inset) Magnification of the lower concentration region of the curves. Data were fit by eq 3 (dashed) and eq 4 (solid). In some cases, error bars are not visible because of the closeness of the values of the replicates.

Figure 8.
Glycine-reduction and reoxidation of PlGoxA. (A) Spectra were recorded of PlGoxA before (black) and after (purple) the addition of glycine. (B) Spectra were recorded of glycine-reduced PlGoxA before (purple) and after exposure to room air. The final spectrum is black and intermediate spectra are shown in the other colors. Arrows indicate the direction of change.
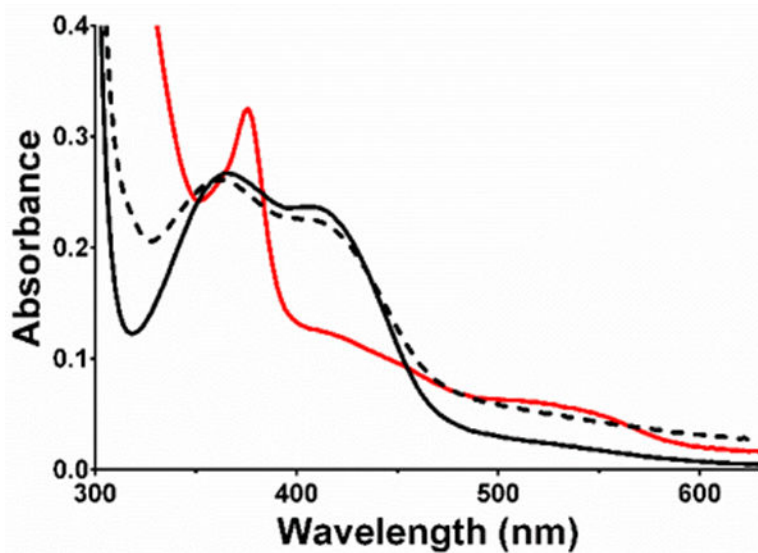
Figure 9.
Dithionite-reduction and reoxidation of PlGoxA. Spectra were recorded of PlGoxA before (black solid) addition of dithionite, after addition of dithionite (red) and after subsequent exposure to room air (black dashed).
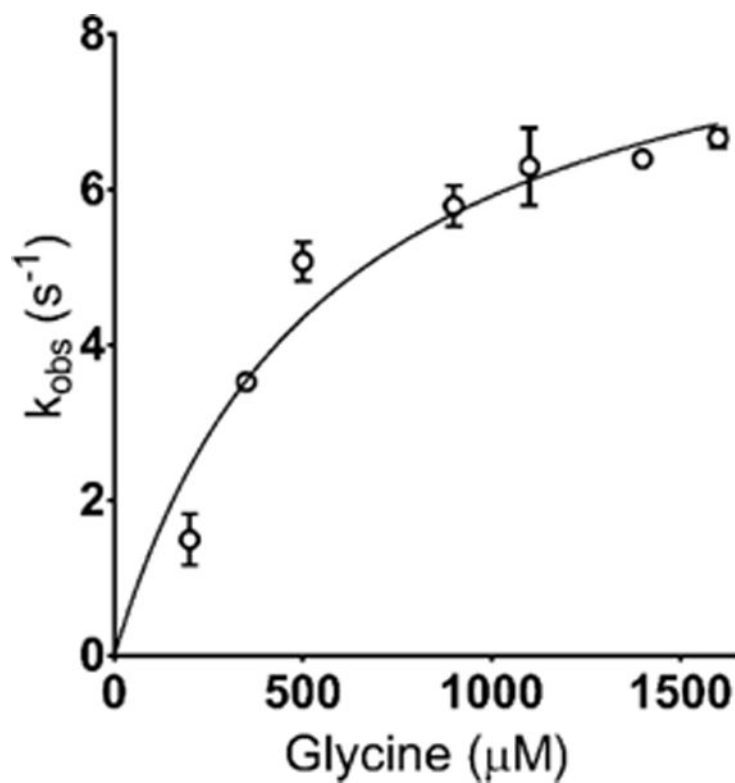
Figure 10.
Single-turnover kinetics of the reduction of CTQ by glycine. Data are fit by eq 6. In some cases, error bars are not visible because of the closeness of the values of the replicates.

Table 1

Distribution of *goxA*-like genes of the Group II LodA-like proteins.

Taxon	Genomes with *goxA*-like genes	Total number of sequenced genomes[a]	Percentage
Proteobacteria[b]	68	24293	0.28
Alphaproteobacteria	53	3196	1.65
Gammaproteobacteria	11	16375	0.06
Betaproteobacteria	4	2596	0.15
Bacteroidetes	8	1979	0.40
Flavobacteria	8	760	1.05
Cyanobacteria	1	426	0.23

[a]Analysis of microbial genome sequences deposited in the IMG database as of July 8, 2017.

[b]Phyla are indicated in bold and classes are indicated in italics.

TABLE 2

Data collection, processing and refinement statistics for PlGoxA

	Native	Pb-SAD
Data collection		
Wavelength (Å)	1.00000	0.95007
Space group	$P2_1$	$P2_1$
Unit cell parameters		
a, b, c (Å)	109.8, 93.2, 188.5	110.8, 93.2, 188.4
α, β, γ (°)	90.0, 94.9, 90.0	90.0, 95.1, 90.0
Resolution range (Å)	48.3 – 2.05	48.4 – 2.36
Number of reflections (measured/unique)	841,420/235,829	262,977/114,759
R_{merge}	0.09 (0.60)	0.06 (0.30)
$I/\sigma I$	10.9 (2.2)	20.3 (2.7)
Completeness (%)	99.3 (97.5)	73.2 (75.9)
Redundancy	3.6 (3.4)	2.3 (2.3)
Refinement Statistics		
Resolution (Å)	2.05	
R_{work}/R_{free}	0.186/0.219	
Number of atoms		
Protein	48,220	
Mg	4	
Water	1,642	
Other	88	
R.m.s. deviations		
Bond lengths (Å)	0.004	
Bond angles (°)	0.780	
Ramachandran Statistics		
Allowed	99.1%	
Outliers	0.9%	
Average B-factor (Å^2)	41.0	